UTHEP-94-0401
April, 1994

AC

Multiple Photon Radiative Effects in $q + (\bar{q})' \to X + H \to X + \gamma\gamma$ At And Beyond LHC Energies*

D. B. DeLaney, S. Jadach,† Ch. Shio, G. Siopsis, and B. F. L. Ward

Department of Physics and Astronomy
The University of Tennessee, Knoxville, TN 37996-1200
U. S. A.

ABSTRACT

We extend our YFS Monte Carlo event generator analysis of $q + (\bar{q})' \to q + (\bar{q})' + n(\gamma)$ to include the production and decay via 2γ of the Standard Model physical Higgs boson H at intermediate Higgs masses 80 GeV $\lesssim m_H \lesssim 2M_W$ at and beyond LHC energies. We find that, for the SDC/GEM/ATLAS/CMS-type cuts, the Higgs signal is very well separated from bremsstrahlung from the fundamental fermions themselves.

*Research supported in part by the Texas National Research Laboratory Commission under grant RCFY-93-347, the DoE under grant DE-FG05-91ER40627, and by Polish Government grants KBN 2P30225206 and KBN 223729102.

†Permanent address: Institute of Nuclear Physics, ul. Kawiory 26a, PL 30-059 Cracow, Poland.

1 Introduction

As the SSC is now essentially shut down, the LHC is still being planned, and, further, discussion has arisen [1] about a possible 60 TeV cms energy upgrade at FNAL. Thus, the era of the large hadron-hadron colliders' exploration of the $SU_{2L} \times U_1$ Standard Model Higgs sector is still alive. It is important to continue to refine the predictions for the various signal and background processes relevant to this exploration to higher and higher precision, so that the extraction of the relevant information from the data will be optimized when these colliders start to produce physics events. At both the LHC and the proposed Super-SSC FNAL upgrade, the Higgs exploration can be mutually divided into the light, intermediate, and heavy Higgs regimes, corresponding respectively to $m_H \lesssim 80$ GeV, 80 GeV $\lesssim m_H \lesssim 2M_W$, $m_H \gtrsim 2M_W$. In the intermediate energy regime, the decay mode $H \to \gamma\gamma$ is expected to play a significant role in the detection strategy for the Higgs; for, in this regime, the gold-plated $H \to$ four leptons events are not available and one needs another relatively clean decay final state to allow the Higgs to be discerned from the ever-present QCD ($SU_{2L} \times U_1$) background processes [2].

Thus, it is an important question as to what are the multiple-photon radiative correction effects to the fundamental process $q + \bar{q}' \to q + \bar{q}' + H$, $H \to \gamma\gamma$, in view of the expected relatively small value of $B(H \to \gamma\gamma)$. Indeed, any significant change in either the normalization or the kinematic variables' profile of this process due to the interplay of multiple-photon radiative effects could endanger the ability of the ATLAS/CMS-type detectors' ability to pick out the Higgs in the intermediate mass regime. In what follows, we use our YFS [3] Monte Carlo (MC) approach to higher order $SU_{2L} \times U_1$ radiative corrections to calculate these multiple-photon effects at LHC energies and at the recently proposed 60 TeV FNAL upgrade energies.

Specifically, we extend the multiple-photon MC SSCYFS2 in Ref. [4], which simulates $q + \bar{q}' \to q'' + \bar{q}''' + n(\gamma)$ processes at or beyond LHC energies, to include the processes $q + \bar{q}' \to q + \bar{q}' + H + n(\gamma)$, $H \to \gamma\gamma$, for m_H in the intermediate mass regime. We use the standard top-quark loop view[5, 6] of the Higgs production and decay, with gluons producing the Higgs in the first such loop and with the Higgs decaying to $\gamma\gamma$ via a second such loop. The large value of m_t, recently evidenced [7] as $m_t = 174 \pm 10^{+13}_{-12}$ GeV, compared to the values of

the other known quarks' masses justifies this use of 1 loops in our calculations. Most of our calculations of numerical results use the central value $m_t = 174$ GeV but we have explored the sensitivity of our results to 1σ variations of m_t for completeness and we comment at the appropriate places on this sensitivity in what follows.

We have in mind that the resulting Higgs production and decay event generator, which we call SSCYFSH, will be ultimately interfaced to an amplitude-based description of either incoming pp or $p\bar{p}$ states, wherein the p and/or $\bar{p}$ are described by Lepage-Brodsky[8] distribution amplitudes. Thus, we treat the fundamental $q + {}^{'}\bar{q}^{'} \to q + {}^{'}\bar{q}^{'} + H + n(\gamma)$, $H \to \gamma\gamma$ process at the level of Feynman diagrams according to our standard YFS[9] MC methods[3]. This does not preclude the use of a parton-model view of the incoming pp or $p\bar{p}$ states and we will present results on such a parton-model realization of the processes $p+p \to q+{}^{'}\bar{q}^{'}+H+X$, $H \to \gamma\gamma$ elsewhere [10]. Here, we focus on the fundamental hard underlying $q+{}^{'}\bar{q}^{'} \to q+{}^{'}\bar{q}^{'}+H+n(\gamma)$, $H \to \gamma\gamma$ processes with the goal of calculating the effects of $n(\gamma)$ radiation at the fundamental level of intermediate Higgs production and decay, both because of its genuine theoretical interest as a property of the QED corrections to such processes and as a basis for calculating the respective corrections to such Higgs processes at the level of the incomping pp or $p\bar{p}$ initial states as well. To repeat, this hadron-hadron-collisions-level discussion will be taken up elsewhere [10].

Our work is organized as follows. In the next section, we review the relevant aspects of the YFS exponentiation formalism which we shall employ and present the extension of our SSCYFS2 MC program to include the intermediate-mass Higgs production and decay to the $\gamma\gamma$ final state. In Section 3, we present some sample MC data from our calculation. Section 4 contains some summary remarks.

2 YFS Exponentiated Higgs Boson Production and Decay

In this section we present the YFS exponentiation of the process $q + {}^{'}\bar{q}^{'} \to q + {}^{'}\bar{q}^{'} + H + n(\gamma)$, $H \to \gamma\gamma$. We begin by a brief review of the relevant aspects of the YFS exponentiation methods that we use.

Specifically, in Ref. [4], we have extended the YFS2 MC methods in Ref. [3], which were developed by two of us for the processes $e^+e^- \to f\bar{f} + n(\gamma)$, $f \neq e$, to the fundamental quark-(anti-)quark scattering processes $q + {}^{(}q^{)'} \to q + {}^{(}\bar{q}^{)'} + n(\gamma)$ at SSC/LHC energies with an eye toward precision background and signal QED radiative corrections to SSC/LHC physics scenarios. From the standpoint of the work in Ref. [4], our current process may be seen as a higher-order correction to the respective Born-level processes considered therein.

Indeed, in Fig. 1, we show the Born-level process, (a), $q + {}^{(}\bar{q}^{)'} \to q + {}^{(}\bar{q}^{)'}$, and, (b), $q + {}^{(}\bar{q}^{)'} \to q\ {}^{(}\bar{q}^{)'} + H$, $H \to \gamma\gamma$, with our presumed dominance of the top-quark loops. Thus, the multiple-photon radiative effects on the latter process may be computed in complete analogy with those on the former, which are currently realized in the YFS exponentiated MC, SSCYFS2. When the $n(\gamma)$ radiative effects are considered, the relevant Feynman graphs, with kinematics, for $q + {}^{(}\bar{q}^{)'} \to q + {}^{(}\bar{q}^{)'} + n(\gamma)$ and $q + {}^{(}\bar{q}^{)'} \to q + {}^{(}\bar{q}^{)'} + H + n(\gamma)$, $H \to \gamma\gamma$ are shown in Fig. 2. Referring to the YFS exponentiation of the former processes in Ref. [4], we see that for both Fig. 2a and Fig. 2b, we have the standard YFS formula

$$d\sigma = e^{2\alpha\, Re\, B + 2\alpha \tilde{B}} \sum_{n=0}^{\infty} \frac{1}{n!} \int \prod_{j=1}^{n} \frac{d^3k_j}{k_j^0} \int \frac{d^4y}{(2\pi)^4} e^{iy(p_1+q_1-p_2-q_2-\sum_j k_j)+D} \bar{\beta}_n(k_1,\ldots,k_n) \frac{d^3p_2 d^3q_2}{p_2^0 q_2^0} \quad (1)$$

where the real infrared function $\tilde{B}$ and the virtual infrared function B are given in Refs. [3, 9, 11], and where we note the usual connections

$$2\alpha\, \tilde{B} = \int^{k \leq K_{max}} \frac{d^3k}{k_0} \tilde{S}(k)$$

$$D = \int d^3k \frac{\tilde{S}(k)}{k^0} \left(e^{-iy\cdot k} - \theta(K_{max} - k) \right) \quad (2)$$

for the standard YFS infrared emission factor

$$\tilde{S}(k) = \frac{\alpha}{4\pi^2} \left[Q_q Q_{{}^{(}\bar{q}^{)'}} \left(\frac{p_1}{p_1 \cdot k} - \frac{q_1}{q_1 \cdot k} \right)^2 + \ldots \right] \quad (3)$$

if Q_f is the electric charge of f in units of the positron charge. Here, the ... represent the remaining terms in $\tilde{S}(k)$ obtained from the one given by respective substitutions of Q_q, p_1, $Q_{{}^{(}\bar{q}^{)'}}$, q_1 with corresponding values for the other pairs of the external fermion legs in Fig. 2 according to the YFS prescription in Ref. [9] (wherein due attention is taken to obtain the correct relative sign of each of the terms in $\tilde{S}(k)$ according to this latter prescription).

The fundamental difference in $\bar{\beta}_n$ for Figs. 2a and 2b lies in the respective $\bar{\beta}_n$ for the two processes. Indeed, for 2b, we need to exhibit the presence of the $H \to \gamma\gamma$ production and decay by writing in (1) the identification

$$\bar{\beta}_n(k_1, \ldots, k_n) = \bar{\beta}'_n(k_1, \ldots, k_n) \frac{d^3\bar{k}_1}{\bar{k}_1^0} \frac{d^3\bar{k}_2}{\bar{k}_2^0} \tag{4}$$

where the two Higgs decay photons have four-momenta $\bar{k}_1$ and $\bar{k}_2$ and satisfy $(\bar{k}_1 + \bar{k}_2)^2 = m_H^2$ when the Higgs is produced on its mass shell. In this intermediate-mass regime which we discuss, we expect the Higgs decay width Γ_H to be small compared to m_H, its rest mass: we take $\Gamma_H \simeq 10$ MeV for $m_H \simeq 150$ GeV. Thus, we do not expect the YFS $n(\gamma)$ radiation from the quark lines, which will be dominated by the gauge-invariant radiation from the top and bottom lines, with radiation times $\sim 1/< k^0 >$, which are therefore much shorter than the decay time $1/\Gamma_H$ of the Higgs, to produce noticeable quantum interference effects between itself and the Higgs decay photons, $\bar{\gamma}_1$ and $\bar{\gamma}_2$ in Fig. 2b, in computing $\bar{\beta}'_n$ in (4). The notation in (4), in which the $\bar{k}_1$, $\bar{k}_2$ dependence of $\bar{\beta}'_n$ is represented as a suppressed dependence, is in complete analogy with that of p_2 and q_2, for example. Here, $< k_0 >$ is the average energy of the YFS photons in Fig. 2b, all of which satisfy $k_0 \geq 3$ GeV by our detector resolution cut parameters. Thus, in order to construct the Higgs extension of our YFS exponentiated MC SSCYFS2 in Ref. [4], we need to compute $\bar{\beta}'_n$ in (4) in accordance with this general calculational framework in which the $n(\gamma)$ and $\bar{\gamma}_{1,2}$ interference effects are dropped due to their small size compared to the dominant non-interference terms in the corresponding expressions for $\bar{\beta}'_n$.

We work to lowest order in the effective interactions which describe the process in Fig. 2b, so that, following the YFS prescription, we get the basic YFS residual as

$$\begin{aligned}
\bar{\beta}'_0 &= d\sigma_B|_{Fig.\ 2b} \\
&= \frac{dE_{k_1}^2\, dE_{k_2}^2}{2^{16}} \frac{d\Omega_{q_1}}{4\pi} \frac{d\Omega_{q_2}}{4\pi} \left(\frac{\alpha_s \alpha m_t^2 q_t}{\pi M_W \sin\theta_W} \right)^4 \frac{1}{t^2 t'^2} \frac{1}{(\mathcal{K}^2 - m_H^2)^2} \\
&\times |2 + (1 - 4\delta_{\mathcal{R}}) F_2(\delta_{\mathcal{R}})|^2 |2 + (1 - 4\delta_{\mathcal{K}}) F_2(\delta_{\mathcal{K}})|^2 \\
&\times \left\{ \mathcal{S}^2 + \frac{1}{2} tt' + tm_2^2 + t'm_1^2 - \frac{1}{\mathcal{R}} \left[2\mathcal{S}UU' + tt'(\mathcal{U} + \mathcal{U}') \right] + \frac{1}{\mathcal{R}^2} \left[tt' + \mathcal{U}^2 \right] \left[tt' + \mathcal{U}'^2 \right] \right\}, \qquad (5)
\end{aligned}$$

where we have defined the kinematic variables

$$\mathcal{S} = s - m_1^2 - m_2^2 = 2p_1 \cdot q_1,\ t = (p_1 - p_2)^2,\ t' = (q_1 - q_2)^2,$$

$t = S + (p_1 - q_2)^2 - m_1^2 - m_2^2 = S - 2p_1 \cdot q_2$, $t' = S + (p_2 - q_1)^2 - m_1^2 - m_2^2 = S - 2p_2 \cdot q_1$

$$\mathcal{K} = k_1 + k_2, \ \mathcal{R} = \mathcal{K}^2 - t - t' \ , \delta_{\mathcal{K}} = m_i^2/\mathcal{K}^2, \ \delta_{\mathcal{R}} = m_i^2/\mathcal{R} \ .$$

$$F_2(x) = -\frac{1}{2}\ln^2\left|\frac{\beta+1}{\beta-1}\right| + \left(\frac{\pi^2}{2} + i\pi\ln\left(\frac{1+\beta}{1-\beta}\right)\right)\theta(x) \ , \quad x < \frac{1}{4}, \quad \beta = \sqrt{1-4x}$$

$$= 2\left[\sin^{-1}\left(1/2\sqrt{x}\right)\right]^2 \ , \quad x > \frac{1}{4} \ . \tag{6}$$

As in Ref. [4], we then use the YFS2 formulas in Ref. [3] to include the leading-log 2nd-order corrections associated with the $n(\gamma)$ radiation from the quark-(anti-)quark legs in Fig. 2b and thereby obtain the complete analog of these corrections as they are already realized in SSCYFS2 (for example, in Ref. [4]). In this way, we arrive at the $\bar{\beta}'_n$ needed to construct the extension of SSCYFS2 to the process in Fig. 2b for H production and decay to $\gamma\gamma$. The corresponding MC event generator is called SSCYFSH and sample data from it at and beyond SSC/LHC energies are illustrated in the next section.

3 Results

In this section, we present sample MC data generated by our SSCYFSH event generator for the process $q + (\bar{q})' \to X + H + n(\gamma) \to X + \gamma\gamma + n(\gamma)$ at LHC energies and beyond. For definitiveness we always show histograms for $\sqrt{s} = 15.4$ TeV for the SDC/GEM/ATLAS/CMS-type acceptance and comment on what happens as well for higher energies. We begin by looking into the number distribution for photons.

Specifically, in Fig. 3, we plot the number distribution for photons in the process $u + u \to u + u + H + n(\gamma) \to u + u + n(\gamma) + \gamma\gamma$, where we require that $k_i^0 > 3$ GeV in the initial $u + u$ cms system for all photon energies k_i^0. What we see is that the $n(\gamma)$ multiple-photon YFS radiation adds a definite tail to the 2γ Higgs decay number distribution which is concentrated at $n = 2$, so that the average number of photons is

$$< n_\gamma > = \ 2.8 \pm 0.9 \ . \tag{7}$$

Entirely similar results hold for $\sqrt{s} = 40$ TeV and 60 TeV. Thus, the immediate questions are what are the effects of this YFS radiation on the respective energy available to produce the

Higgs and on the corresponding H cross section mass distribution. We first turn to the energy radiated into initial-state photons.

We investigate the energy radiated into the initial state photons by analyzing the distribution of the variable $v = (s - s')/s$ in our process $u + u \to u + u + H + n(\gamma) \to u + u + n(\gamma) + \gamma\gamma$. Here $s\,(s') = (p_1 + q_1)^2$ $((p_2 + q_2)^2)$ as usual. This is shown in Fig. 4 for $\sqrt{s} = 15.4$ TeV. (A similar plot pertains to $\sqrt{s} = 60$ TeV.) What we see is that the average value of v is

$$< v > = \ 0.30 \pm 0.23 \ . \tag{8}$$

Thus, a significant amount of radiation is taken away from the interaction by the $n(\gamma)$ system. This means that the cross section for H production will be affected in general by $n(\gamma)$ radiation and we find the normalization of our cross section is indeed changed by

$$\delta\sigma/\sigma_B = (6.9 \pm 0.6)\% \tag{9}$$

relative to its Born-level value by the $n(\gamma)$ radiative effects.

Turning next to the fundamental $\gamma\gamma$ mass distribution itself in our proto-typical process $u + u \to u + u + H + n(\gamma) \to u + u + n(\gamma) + \gamma\gamma$, we plot it in Fig. 5. What we see is that the $n(\gamma)$ radiation produces a tail on the $\gamma\gamma$ peak which is most prominent at values of $M_{\gamma\gamma} < m_H$, where m_H is 150 GeV here for definiteness. From the inset plot of the region near m_H in Fig. 5, however, we see that the fundamental fermion radiation background is at the level of .1% so that it is well below the expected $\sim 3GeV$ resolution of the LHC-type detectors in its effects on the observed mass and width of the Higgs. Hence, the Higgs signal is not obscured very much at all by this fundamental fermion $n(\gamma)$ radiation. One gets an entirely similar conclusion at $\sqrt{s} = 60$ TeV, for example. This is encouraging for the use of the $H \to \gamma\gamma$ decay as an intermediate Higgs discovery channel.

Our main conclusions in this section are therefore that $n(\gamma)$ radiative effects must be taken into account to understand the normalization of the processes $q + {}^{(}\bar{q}{}^{)\prime} \to q + {}^{(}\bar{q}{}^{)\prime} + H + n(\gamma)$, $H \to \gamma\gamma$ at and beyond LHC energies and that $\Delta M_{\gamma\gamma}$, the width of the $M_{\gamma\gamma}$ distribution at $M_{\gamma\gamma} = m_H$ due to $n(\gamma)$ radiative effects, is indeed small at such energies and does not represent a serious impediment to intermediate-mass H discovery in the $H \to \gamma\gamma$ channel.

4 Conclusions

In this paper, we have investigated the interplay between the multiple photon YFS radiation and the $H \to \gamma\gamma$ decay photons in the processes $q + \bar{q}' \to q + \bar{q}' + H + n(\gamma)$, $H \to \gamma\gamma$ at LHC energies. We did this by extending our YFS MC event generator SSCYFS2 to include the Higgs production and decay to 2 photons. Our results are encouraging for the use of the $H \to \gamma\gamma$ channel for intermediate-mass H discovery.

Specifically, we find that the mean number of YFS soft photons produced in the process $u + u \to u + u + n(\gamma) + H \to u + u + n(\gamma) + \gamma\gamma$ is $< n_\gamma > = 2.8 \pm 0.9$. The average value of the parameter $v = (s - s')/s$ for these photons is $< v > = 0.30 \pm 0.23$, with a corresponding normalization effect of $\Delta\sigma/\sigma_B = (6.9 \pm 0.6)\%$. Hence, these $n(\gamma)$ photons must be taken into account for a precise description of the intermediate-mass Higgs production and decay to two photons in the LHC and higher-energy environments. We also find that the $\gamma\gamma$ mass distribution is only mildly affected, at the level of .1%, in the region of m_H in the LHC-type environment, for $m_H = 150$ GeV, so that the $n(\gamma)$ radiation does not render the H inaccessible in the $\gamma\gamma$ mass plot. Thus, our results support the use of this $H \to \gamma\gamma$ channel for intermediate Higgs mass exploration at and beyond LHC energies.

We conclude that multiple YFS soft-photon radiative effects do not mask the intermediate Higgs discovery and exploration via its 2-photon decay mode in the LHC-type environments. Such effects must be taken into account for precision studies of this channel, however, and our SSCYFSH MC event generator affords a convenient method of realizing such effects in the presence of arbitrary detector cuts. It is available from the authors upon request.

Acknowledgements

The authors are very much indebted to Profs. F. Gilman and W. Bardeen of the former SSCL for their kind hospitality while a part of this work was done. Two of the authors (S. J. and B. F. L. W.) are indebted to Prof. John Ellis of the CERN TH Division for his kind hospitality while this work was conceived and initiated. The authors thank Dr. E. Richter-Was for useful

discussion.

References

[1] G. Foster, talk at Drell Panel Town Meeting, 1994.

[2] See, for example, J. F. Gunion, G. L. Kane, and J. Wudka, *Nucl. Phys.* ***B299***, 231 (1988), and references therein.

[3] S. Jadach and B. F. L. Ward, *Comp. Phys. Comm.* ***56***, 351 (1990), and references therein.

[4] D. B. DeLaney *et al.*, *Phys. Rev.* ***D47***, 853 (1993); *Phys. Lett.* ***B292***, 413 (1992); *ibid.* ***B302***, 540 (1993).

[5] See, for example, D. Graudenz, M. Spira, and P. M. Zerwas, *Phys. Rev. Lett.* ***70***, 1372 (1993).

[6] R. P. Kauffman, *Phys. Rev.* ***D49***, 2298 (1994); S. Dawson, *Nucl. Phys.* ***B359***,283 (1991), and references therein.

[7] F. Abe *et al.*, FERMILAB-PUB-94-116-E, May, 1994.

[8] G. P. Lepage and S. J. Brodsky, *Phys. Rev.* ***D22***, 2157 (1980).

[9] D. R. Yennie, S. C. Frautschi, and H. Suura, *Ann. Phys. (NY)* ***13***, 379 (1961).

[10] S. Jadach, *et al.*, to appear.

[11] B. F. L. Ward, *Phys. Rev.* ***D36***, 939 (1987); *ibid.* ***D42***, 3249 (1990).

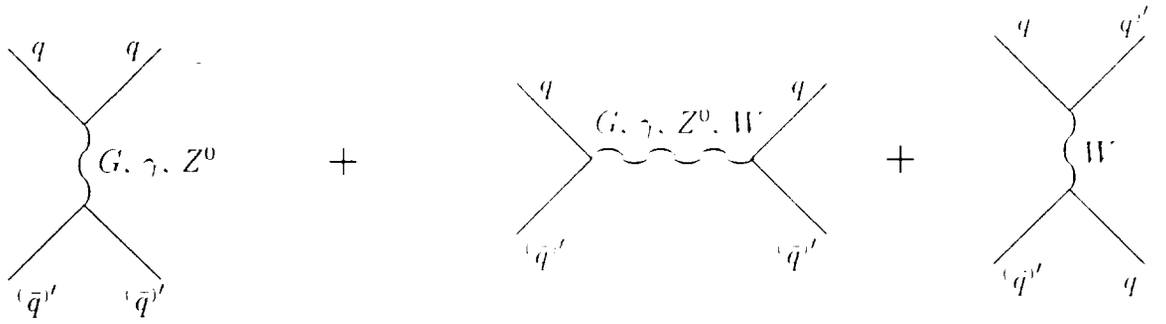

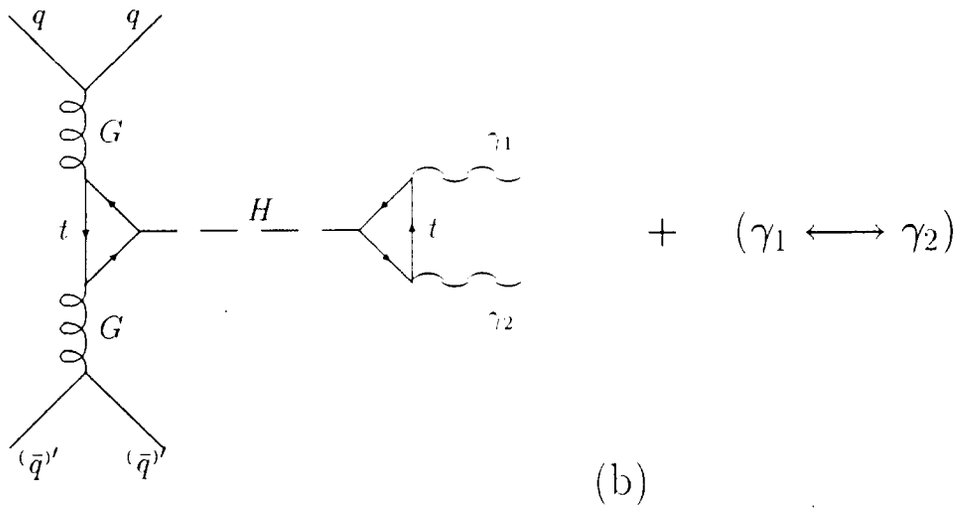

Figure 1: (a). Born graphs for $q + {}^{(}\bar{q}{}^{)\prime} \rightarrow q + {}^{(}\bar{q}{}^{)\prime}$. (b). Lowest order graphs for $q + {}^{(}\bar{q}{}^{)\prime} \rightarrow q + {}^{(}\bar{q}{}^{)\prime} + H \rightarrow q + {}^{(}\bar{q}{}^{)\prime} + \gamma\gamma$.

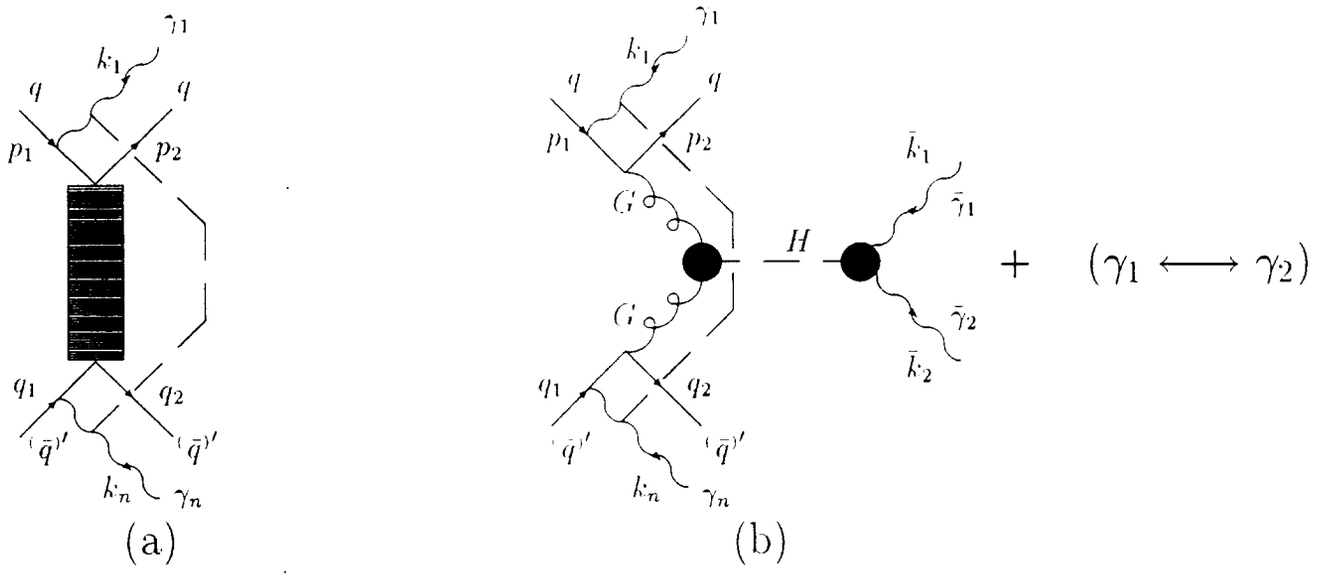

Figure 2: (a). The process $q + (\bar{q})' \rightarrow q + (\bar{q})' + n(\gamma)$. (b). The process $q + (\bar{q})' \rightarrow q + (\bar{q})' + H + n(\gamma) \rightarrow q + (\bar{q})' + \bar{\gamma}_1\bar{\gamma}_2 + n(\gamma)$, where $\bar{\gamma}_i$ are the H decay photons. The four-momenta are indicated in the standard manner: p_1 is the four-momentum of the incoming q, p_2 is the four-momentum of the outgoing q, etc.

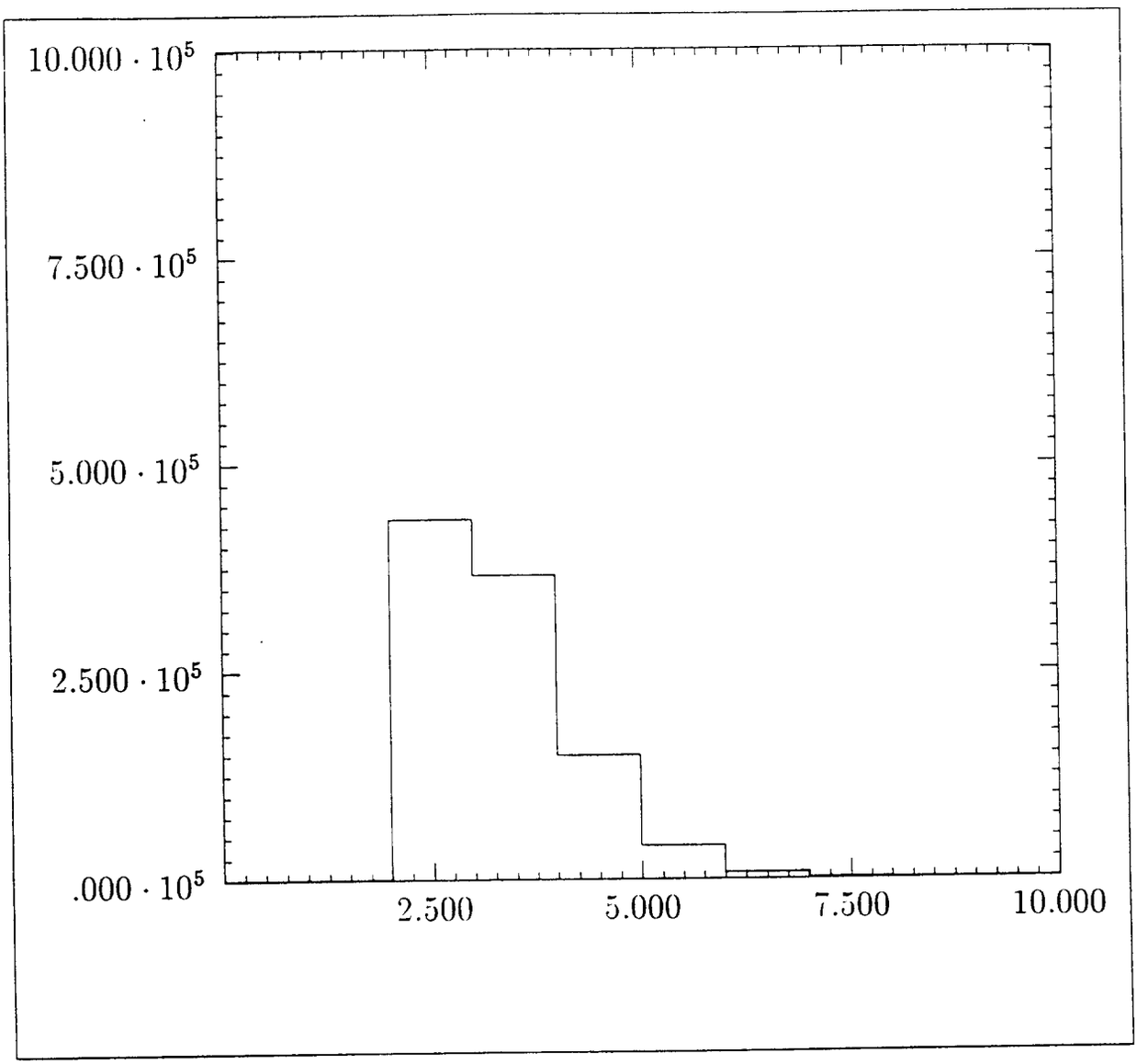

Figure 3: Photon number distribution for $u + u \to u + u + H + n(\gamma) \to u + u + \bar{\gamma}_1\bar{\gamma}_2 + n(\gamma)$, for $E_\gamma > 3$ GeV in the incoming uu c.m.s. system at $\sqrt{s} = 15.4$ TeV.

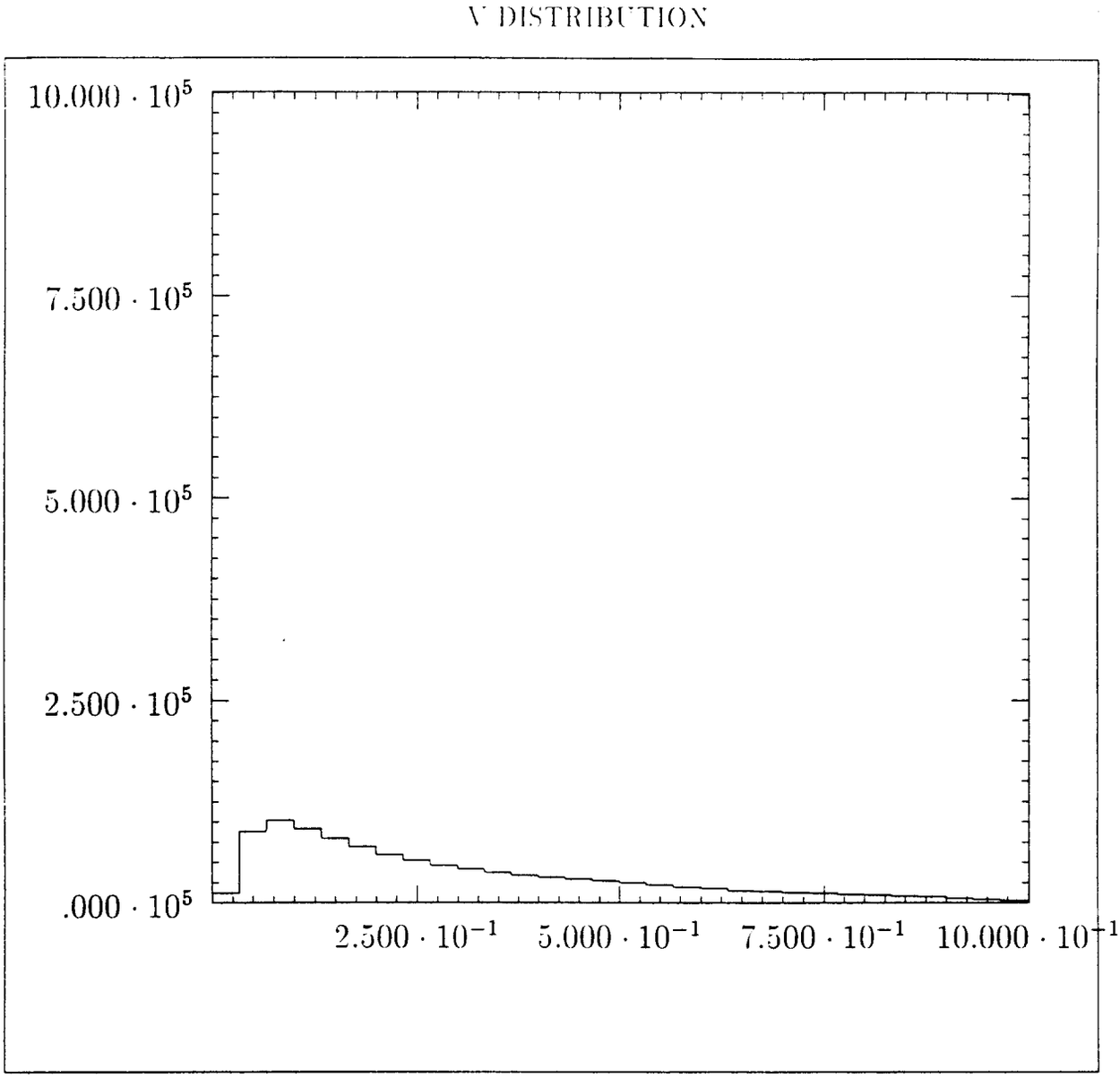

Figure 4: v–distribution for the process $u + u \to u + u + H + n(\gamma) \to u + u + \bar{\gamma}_1\bar{\gamma}_2 + n(\gamma)$ at $\sqrt{s} = 15.4$ TeV.

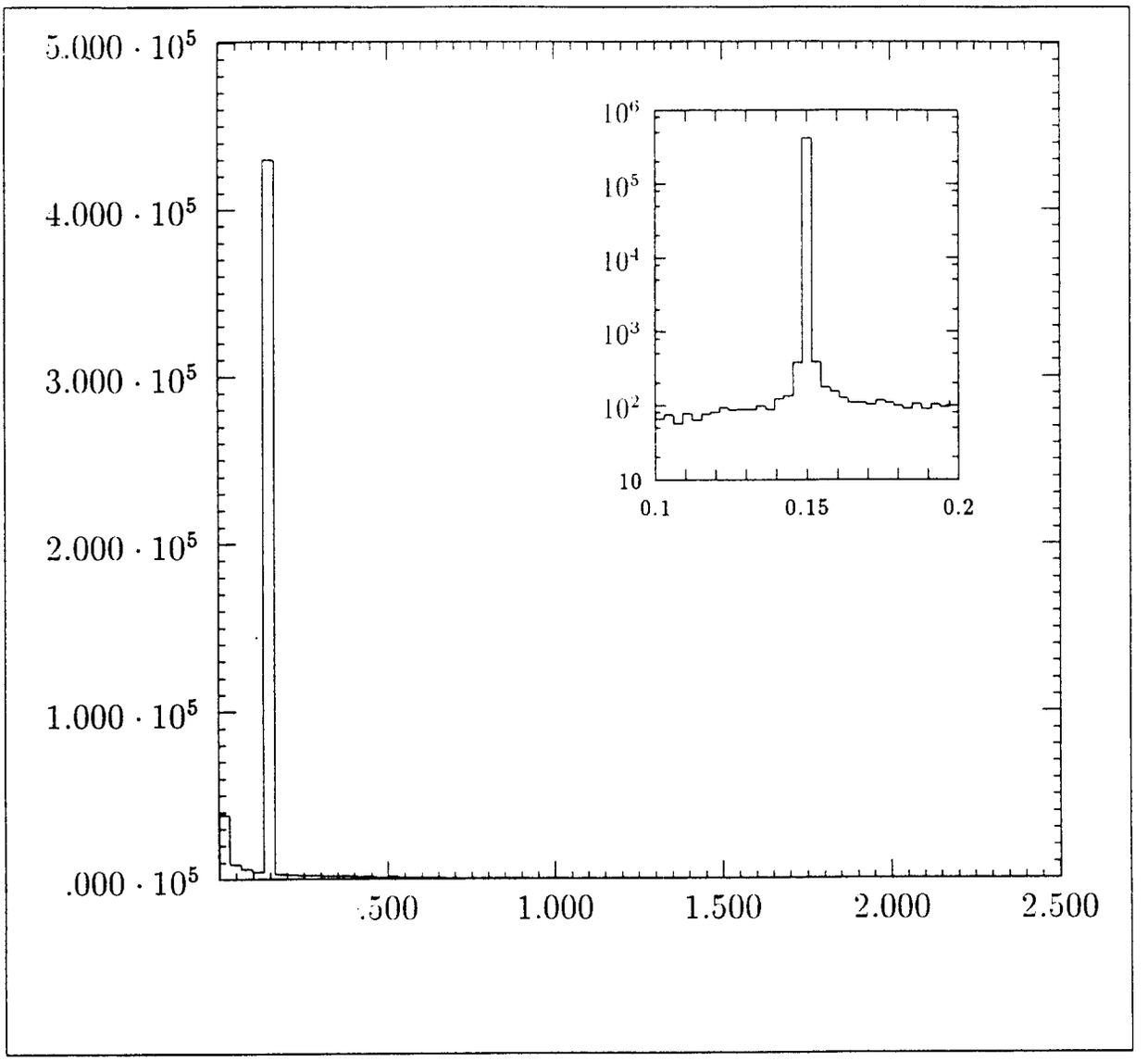

Figure 5: $\gamma\gamma$-mass distribution for the process $u + u \to u + u + H + n(\gamma) \to u + u + \bar{\gamma}_1\bar{\gamma}_2 + n(\gamma)$ at $\sqrt{s} = 15.4$ TeV.